Investigation of Slag Compositions and Pressure Ranges suitable for Electroslag Remelting under Vacuum Conditions

S. Radwitz[1], H. Scholz[2], B. Friedrich[1]
[1]IME Process Metallurgy and Metal Recycling, RWTH Aachen University, D-52056 Aachen, Germany
[2]ALD Vacuum Technologies GmbH, Wilhelm-Rohn-Strasse 35, D-63450 Hanau, Germany

Keywords: ESR slags, oxygen content, refining of steel, vacuum conditions

Abstract

It is well known that high contents of oxygen and hydrogen in creep resistant structural steels like 21CrMoV5-7 have negative influence on a variety of material properties. To investigate the refining ability of various slag compositions under reduced pressure multiple experiments were performed in a 40 kW vacuum-induction furnace with the aim to ensure minimal oxygen and hydrogen contents. With regard to slag evaporation, different mixtures of fluorides and oxides as well as pure oxide systems were utilized. The pressure was varied in the range of 5 and 700 mbar.
The behavior of different slags under vacuum conditions as well as the results of various chemical analysis were used to evaluate the application of the investigated slag systems for ESR under vacuum conditions. Special attention was given to easily oxidizable alloy elements as aluminum and silicon, the amount of oxygen and hydrogen as well as on formation of non-metallic inclusions.

Introduction

The presence of non-metallic inclusions (NMIs) in metallic materials results in the occurrence of rolling and surface defects during further processing as well as in a decrease of the mechanical properties and corrosions resistance.
Thereby, the effect of NMIs on the material behavior depends strongly on their size, morphology, distribution and chemical composition. For instance, the fracture toughness and ductility are greatly reduced with an increasing content of oxides and sulfides. In addition, brittle oxide components (e.g. Al_2O_3 inclusions) could serve as potential crack initiators. [1]
Due to the fact that a dominating factor with regard to the amount of non-metallic inclusions consists in the content of dissolved oxygen in liquid steel, it is of interest to minimize the total oxygen (T.O.) content by various metallurgical treatments. According to that, Zhang and Thomas [2] have summarized typical steel cleanliness requirements, published by various authors, for common steel grades (cf. Table I).

Table I: Steel cleanliness requirements for various steel grades [2]

Product class	Maximum impurity fraction in ppm	Maximum inclusion size in µm
Tinplate	T.O. < 20, C < 30, N < 30	20
Tube seel	T.O. < 30, N < 35, S < 30	100
Ball bearing steels	T.O. < 10	15
Heavy plate steels	T.O. < 20, H < 2, N < 30-40	13 (Single inclusions) 200 (Cluster)
Tire cord	T.O. < 15, H < 2, N < 40	10-20
Wire rod	T.O. < 30, N < 60	20

Fundamentals

In the ESR process, a consumable electrode is continuously melted in a water cooled cooper mold while being inserted into a liquid slag bath. On the electrode tip, liquid metal droplets are formed which sink through the slag bath after detaching from the electrode. After passing the slag, the droplets are collected in a typical U-shaped liquid metal pool before solidifying as the remelted ingot (cf. Figure 1).

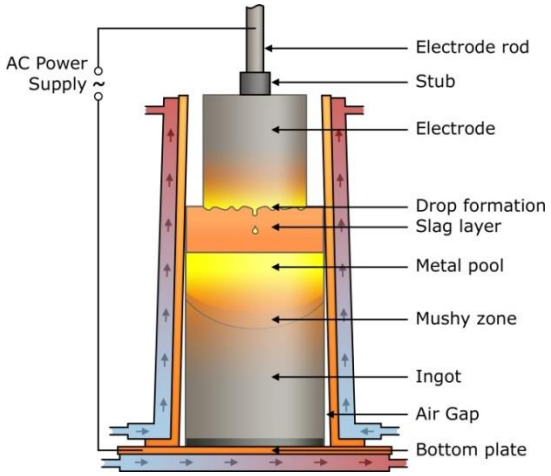

Figure 1: Schematic procedure of the ESR process [3]

In the ESR process various chemical and physical interdependencies between the remelted material (alloying elements, dissolved interstitial elements and non-metallic inclusions), the cat- and anions of the slag system and the gas atmosphere are present. An appropriate illustration of these interactions is given by Figure 2.

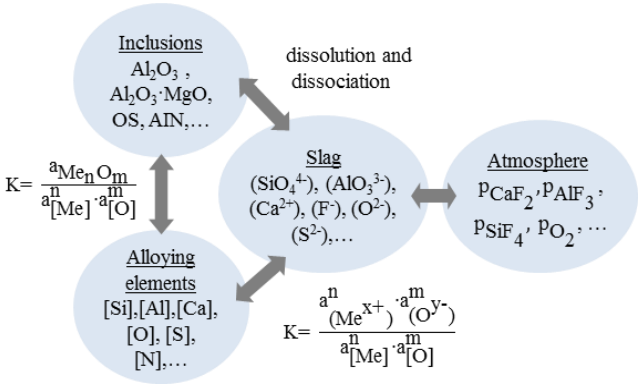

Figure 2: Chemical and physical interactions between alloy, slag and atmosphere during ESR [4]

It could be seen that one influencing factor on the oxygen content of the steel melt is given by the amount of dissolved elements with a high affinity for oxygen such as calcium, aluminum or silicon. On the one hand a reaction of these metals with oxygen would therefore result in a decreased oxygen content and oxygen activity respectively but on the other hand would also generate oxide inclusions which need to be removed from the liquid steel (cf. Equation 1-3).

$$2\,[Al]_{steel} + 3\,[O]_{steel} \leftrightarrow <Al_2O_3> \quad (1)$$

$$[Si]_{steel} + 2\,[O]_{steel} \leftrightarrow <SiO_2> \quad (2)$$

$$[Ca]_{steel} + [O]_{steel} \leftrightarrow <CaO> \quad (3)$$

Since these forming oxides are hardly soluble in the steel melt their activity could be considered as one.
Thus, the general expression of the equilibrium constant for one of the reactions above (cf. Equation 4) could be simplified to the so-called deoxidation constant (cf. Equation 5).

$$K_{Me_xO_y} = \frac{a_{<Me_xO_y>}}{a^x_{[Me]_{steel}} \cdot a^y_{[O]_{steel}}} \quad (4)$$

$$K'_{Me,O} = a^x_{[Me]_{steel}} \cdot a^y_{[O]_{steel}} \quad (5)$$

According to Henry's law, the activity of a dissolved element in a dilute solution is given by Equation 6.

$$a_i = f_i \cdot x_i \quad (6)$$

In order to calculate the according concentration equilibria, the method using interaction coefficients (e_i^j) presented by Wagener [5] could be utilized reliably for low alloyed steels. The Henrian activity coefficients could therefore be expressed by Equation 7.

$$\log f_i = \sum_i^n (e_i^j \cdot [\%j]) \quad (7)$$

As a result of such considerations, the correlation between dissolved oxygen, alloying elements and their corresponding oxides leads to the typical curve progression illustrated by Figure 3.

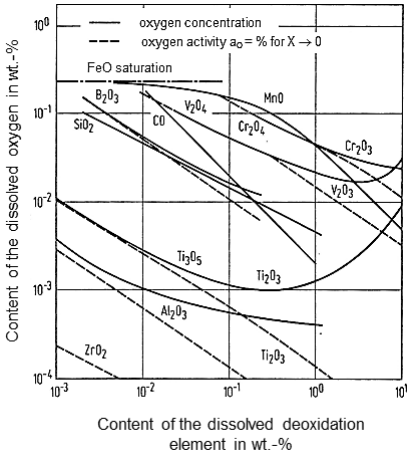

Figure 3: Equilibria between oxygen and various deoxidizing elements dissolved in liquid iron at 1600 °C [6]

At this point, it should be noted that in the ESR process such reactions mainly occur during solidification in the mushy zone (if no deoxidizing elements are added during remelting).
If this kind of new formed inclusions are able to reach the interface between the slag bath and the liquid metal pool by flotation (which is discussed controversial in literature [7]) they could be dissociated and absorbed by the slag. However, inclusions contained already in the electrode material could be removed more effectively at the various reaction zones between the liquid metal and the slag bath.

Another important factor determining the oxygen content of the steel is found in the interaction of the metallic melt and the liquid slag bath. Since in the case of electroslag remelting the common utilized slag systems are based on calcium fluoride with additions of comparatively stable oxides such as CaO, Al_2O_3 or MgO, the cleanliness of the metal is greatly affected by the oxygen activity as well as by the activity of inclusion-forming elements. Under these circumstances the expression for the equilibrium constant for the reaction between an alloying element and oxygen (cf. Equation 8) has to be modified as shown by Equation 9.

$$x\,[Me]_{steel} + y\,[O]_{steel} \leftrightarrow [Me_xO_y]_{slag} \quad (8)$$

$$K_{Me_xO_y} = \frac{a_{[Me_xO_y]_{slag}}}{a^x_{[Me]_{steel}} \cdot a^y_{[O]_{steel}}} \quad (9)$$

As could be seen the activities of slag components are of great importance for determining the appropriate equilibrium constants. With regard to the correlation given in Figure 3, a decrease of the oxide activity by dissolving it in the slag ($a_{[MeO]slag} < 1$) would lead to a shift of equilibrium towards smaller dissolved contents of oxygen and deoxidizing elements in the steel.
In this case, especially the availability of data for oxide activities in fluoride based slags is very limited in the current literature. Referring to pure oxide systems, consisting mainly of CaO and Al_2O_3, Riyahimalayeri [8] et al. have summarized different approaches for calculating the activity of Al_2O_3. Further suggestions of Mitchell [9] include the assumption for systems containing less than 70 wt.-% CaF_2 that calcium fluoride could be considered as an inert diluent.

In addition to the influence on the oxygen content of the metal various reactions with slag components could result in a loss of alloying elements as exemplified by Equation 10.

$$3\,[Si]_{steel} + 2\,[Al_2O_3]_{slag} \leftrightarrow 2\,[Al]_{steel} + 3\,[SiO_2]_{slag} \quad (10)$$

Besides to the contact with the liquid metal, the slag system is also driven to reach equilibrium with the gas phase.
Due to the high process temperatures fluoridic components are continuously evaporating as illustrated by Equation 11 and 12.

$$[CaF_2]_{slag} \leftrightarrow \{CaF_2\} \quad (11)$$

$$3\,[CaF_2]_{slag} + [Al_2O_3]_{slag} \leftrightarrow 3\,[CaO]_{slag} + 2\,\{AlF_3\} \quad (12)$$

The corresponding vapor pressure curves of selected components (cf. Figure 4) show that the evaporation of the present oxides is negligible compared to that of existing and forming fluorides.

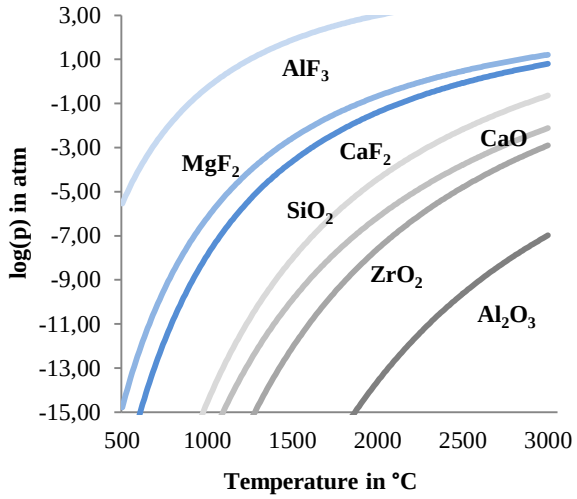

Figure 4: Correlation of vapor pressure and temperature for selected components (calculated with FactSage 6.3 [10])

Due to the fluoride evaporation the electroslag remelting is usually performed under normal or overpressure. To minimize the oxidative loss of alloying elements as well as the introduction of oxygen into the liquid metal a protective argon atmosphere could be applied. However, the findings of Saito et al. [11] and Sekiya et al. [12] indicate the possibility to achieve very low contents of oxygen (approximately 10 ppm) and non-metallic inclusions by carrying out the remelting under vacuum conditions in the range of 66 to 200 mbar.

Experimental Work

Since numerous factors are influencing the total oxygen content of a remelted steel the focus of the present work lies on the investigation of chemical interactions between metal and slag as well as on the slag behavior under reduced pressure. Therefore, a specific steel grade was melted under various slag compositions and pressure ranges in a lab scale vacuum induction furnace. Basing on these results subsequent remelting trials will be carried out as a next step to further examine factors determining the final oxygen content of the metal but are not part of the current work.
The performed investigation involves nine slag treatments of the creep resistant structural steel 21CrMoV5-7 as well as the sampling and analysis of metal and slag after each trial. Prior vacuum induction melting, the chemical composition of the used steel grade was analyzed by optical emission spectroscopy as well as by using combustion and inert gas fusion methods (cf. Table II and III).

Table II: Chemical composition of the utilized steel 21CrMoV5-7 in wt.-%

C	Si	Mn	Al	Cr
0.20	0.273	0.671	0.017	1.288

Mo	Ni	V	Zr
0.710	0.486	0.279	0.0015

Table III: Total content of interstitial elements in ppm

S	O	N	H
18	42	66	2

Vacuum Induction Melting

The melting was carried out in a 40 kW and 10 kHz lab scale induction furnace (cf. Figure 5) which is equipped with various devices for material charging, temperature measurement and sampling via a lock.

Figure 5: Utilized vacuum induction furnace at IME

To investigate the refining potential of different slag compositions with regard to the oxygen content of the steel, various mixtures of a premelted calcium-aluminate slag as well as of prefused fluorspar were blended. In this case, the oxidic slag contains equal amounts of alumina and lime. However, due to the conditions of manufacturing the slag also includes approximately five percent magnesia. The fluorspar has a purity of at least 97 wt.-% CaF_2. Moreover, the main impurities contained therein also consist of alumina and lime.
For all slag treatments, at least two different pressures inside the furnace chamber were applied. To minimize the influence of atmospheric oxygen on the total oxygen content of the metal the furnace chamber was evacuated at least to a pressure below 10^{-2} mbar before heating-up under a protective argon atmosphere with 700 mbar. An overview of the performed trials is given in Table IV.

Table IV: Performed VIM trials with variation of slag composition and process pressure

Trial	Utilized slag compositions	Pressure in mbar
T1	46.9 % CaO, 46.6 % Al_2O_3, 5.0 % MgO	700
T2	46.9 % CaO, 46.6 % Al_2O_3, 5.0 % MgO	200
T3	46.9 % CaO, 46.6 % Al_2O_3, 5.0 % MgO	7
T4	20 % CaF_2, 37.4 %CaO, 37.1 %Al_2O_3, 4.0 % MgO	700
T5	20 % CaF_2, 37.4 %CaO, 37.1 %Al_2O_3, 4.0 % MgO	5
T6	80.0 % CaF_2, 9.5 %CaO, 9.4 %Al_2O_3, 0.9 % MgO	700
T7	80.0 % CaF_2, 9.5 %CaO, 9.4 %Al_2O_3, 0.9 % MgO	5
T8	97.0 % CaF_2, 1.5 %CaO, 1.5 %Al_2O_3	700
T9	97.0 % CaF_2, 1.5 %CaO, 1.5 %Al_2O_3	5

As crucible material densely sintered zirconia (yttria-stabilized) was utilized due to the comparatively slow dissolution rate in the fluoride based slag. Furthermore, to minimize the reaction time between crucible and slag, the prior blended slag components were added on top of the metal melt via the lock. Once the slag was completely melted, the pressure was reduced in the corresponding trials until an extensive bubbling of the slag was observed. Independent of the fluorine content, this phenomenon constantly occurred when reaching a pressure of 5 mbar.

In contrast to the ESR process, where remelting is performed in a water-cooled cooper mold, the liquid metal is subjected to chemical interactions with the oxidic crucible material (cf. Equation 13).

$$<ZrO_2> \leftrightarrow [Zr]_{steel} + 2\,[O]_{steel} \quad (13)$$

However, according to the equilibrium position of the reaction above (cf. Figure 3), the equilibrium content of oxygen which is due to pick up from the crucible is only in the range of 2 ppm at 1600 °C.

By melting in an induction field heat is generated directly in the metal and only marginal in the slag. In order to prevent distinct temperature differences between metal and slag the crucible was placed in a tubular graphite susceptor (cf. Figure 6). Thereby, sticking of slag particles on the crucible wall was also avoided.
With an inner diameter of 59 mm and a height of 93 mm, the utilized crucibles had a maximum filling volume of 220 ml. To keep the ratio between metal and slag constant in all trials approx. 790 g of metal and 103 g of slag were used. Hence, the crucible was half filled with liquid steel and to a quarter with liquid slag. In T1-T3 smaller crucibles had to be used with an inner diameter of 44 mm and a height of 73 mm but the ratio between metal and slag was equal to the other trials.

Figure 6: Arrangement of the experimental set-up

During the trials the temperature was measured using platinum-rhodium thermocouples by two different methods. One thermocouple was centrically placed below the bottom of the crucible. The second measurement was performed periodically by immersion measurements via the lock. Both measurements showed a metal temperature of approx. 1550 °C whereas the slag temperature was at least 50 °C lower.

In order to prevent an extensive mixing of slag and metal during casting, the material was allowed to solidify in the crucible. Thus, every trial required the use of a new crucible.

After melting, slag and vacuum treatment respectively, the obtained ingots were sectioned and sampled in the mechanical workshop at IME and characterized by the same methods as the input material. Referring to Figure 7, the optical emission spectroscopy was carried out by analyzing the blue illustrated parts. The combustion and inert gas fusion techniques were applied to the yellow highlighted sections.

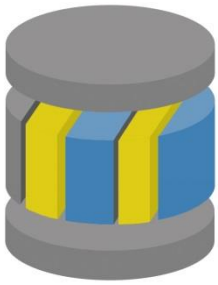

Figure 7: Sampling of the metal ingots

Results and Discussion

After each trial a strong adhesion of the utilized slag on the crucible wall was observed (cf. Figure 8, up). As expected the received metal ingots contained noticeable shrinkage cavities at the bottom and the side walls (cf. Figure 89, down).

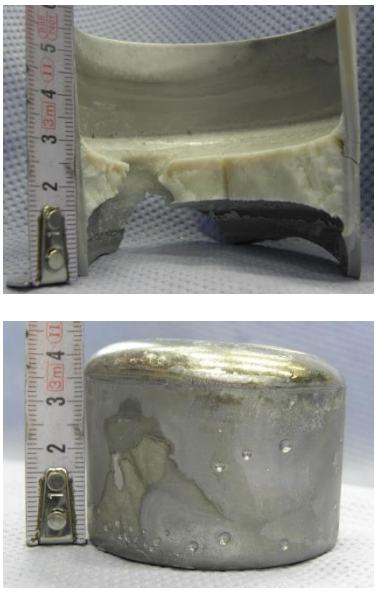

Figure 8: Representative illustration of the received slag layer attached to the crucible (up) and the obtained metal ingot (down)

A selection of analyzed elements via optical emission spectroscopy is given in Table V. For the additional elements (Cr, Ni, Mo and V) listed in Table II no significant differences to the contents of the input material were found.
With respect to the proportion of silicon a decrease was detected after treatment with all slags containing oxides in a notable quantity (T1-T7). Within these, the silicon loss was most distinct when the metal was interacting with a pure oxide slag. With an increasing amount of calcium fluoride the silicon loss could be reduced significantly. Furthermore, by utilizing a technically pure

CaF_2-slag (T8, T9), the silicon content of the metal was fully retained.
Simultaneously to the decrease of silicon, an increase of the aluminum content was observed in all trials containing Al_2O_3 as slag component. These findings could be explained by the high alumina and low silica activity in the slag resulting in the reaction given in Equation 10. Additionally, it is noticeable that only the use of a pure fluoridic slag results in a comparatively strong decrease of the aluminum content. Referring to the deoxidation equilibrium of oxygen and aluminum, a possible explanation for that could be found in the greatly reduced alumina activity in the slag.
Additionally, with the utilization of Fact Sage 6.3 [10] a first approach of estimating the loss of silicon and the increase of the aluminum content was performed using FSstel and FToxid databases. Since under these circumstances only a reliable simulation of the interaction between steel and a solely oxidic slag is possible, the calculations were limited to T1-T3. In good agreement with the present findings a resulting silicon amount of 0.217 wt.-% was calculated for equilibrium conditions between steel and slag. However, the according aluminum content of 0.078 wt.-% was significantly higher than the measured values. On the one hand this amount is consistent with the trend observable in T4-T9 but on the other hand indicates to low aluminum contents in T1-T3.
The low manganese losses could either be the result of metal-slag reactions or slight evaporation effects.
By considering the amount of zirconium an increase was observed in all trials but much more intense when the slag treatment was performed under reduced pressure. However, a correlating variation of the resulting oxygen content in the metal was not detected. Since the dissociation of ZrO_2 is nearly not depending on pressure, the deviation of the measured values is suspected to be due to the inaccuracy of the analyzing method in the present concentration range. Additional calculations using FactSage 6.3 [10] analogously showed an equilibrium concentration of approx. 0.02 % Zr in the according steel melt while being in contact with solid ZrO_2 at 1550 °C. A simultaneous rise of the dissolved oxygen content was also not observable by that simulation.
At this point it should be noted the increased carbon content in T4 is due to an unintended immersion of the graphite tube in the steel melt which was used as protection cover for the submerged thermocouple.

Table V: Analysis of selected elements after slag treatment compared to the input material

	C	Si	Mn	Al	Zr
Input material	0.203	0.273	0.671	0.017	0.0015
T1	0.180	0.204	0.642	0.022	0.0023
T2	0.200	0.223	0.640	0.040	0.0022
T3	0.190	0.186	0.645	0.021	0.0017
T4	0.444	0.224	0.664	0.049	0.0082
T5	0.200	0.217	0.659	0.057	0.011
T6	0.208	0.248	0.667	0.037	0.0042
T7	0.198	0.248	0.665	0.038	0.011
T8	0.202	0.276	0.653	0.0067	0.0037
T9	0.203	0.281	0.651	0.0066	0.028

The according contents of the interstitial or inclusion forming elements are given in Table VI. Due to the content of calcium oxide in the slag it was possible to further reduce the sulfur fraction below 10 ppm, even in the trials T8 and T9. With regard to nitrogen a decreasing pressure resulted in reduced amounts in T1-T3. In the further trials T4-T9 no significant differences with respect to the resulting nitrogen content were found.
Similar observations were made when considering the hydrogen contents. For the trials T1-T3 it was not possible to influence the hydrogen content significantly by the combined vacuum-slag treatment. However, in T4-T9 the hydrogen content was further reduced to values below 1 ppm.

Table VI: Analysis of interstitial elements after slag treatment compared to the input material

	S	O	N	H
Input material	18	42	66	2
T1	< 10	19.2	73	1.78
T2	< 10	15.2	31	1.81
T3	< 10	9.8	16	1.7
T4	< 10	6	14	0.7
T5	< 10	6	12	0.6
T6	< 10	5	16	0.7
T7	< 10	8	16	0.7
T8	< 10	6	6	0.8
T9	< 10	7	12	0.8

Furthermore, T1-T3 showed that it was possible to reduce the total oxygen content of the metal by decreasing the process pressure when melting under a pure oxide based slag (cf. Figure 9). In contrast to that, all trials including CaF_2 as slag component resulted in even lower oxygen contents between 5 and 8 ppm. A dependency on the process pressure could not be observed

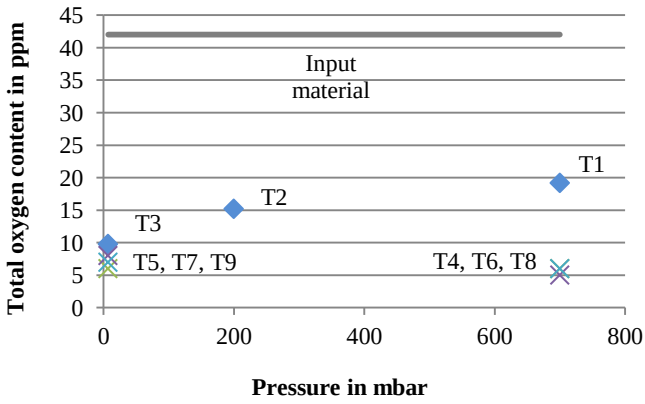

Figure 9: Correlation between the total oxygen content of the metal and the applied pressure compared to that of the input material

By considering the equilibria between oxygen and aluminum as well as between oxygen and silicon it could be concluded that the measured oxygen contents are clearly below those of the silicon deoxidation equilibrium. However, referring to the interaction of oxygen and aluminum, the analyzed contents noticeably exceed

the corresponding equilibrium amounts at process temperature of 1550 °C even by assuming an alumina activity of one as shown in Figure 10.

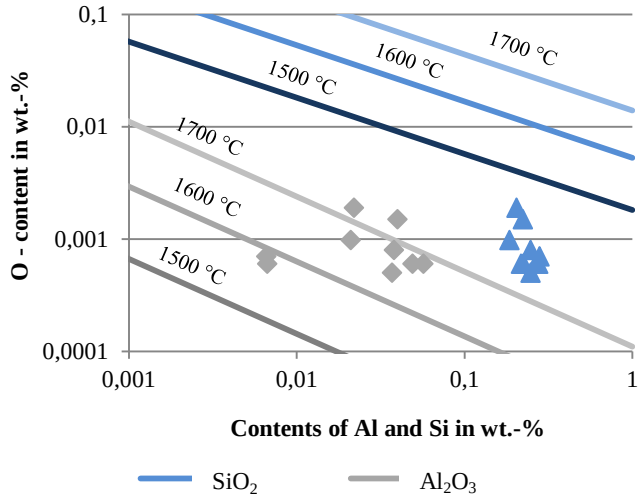

Figure 10: Equilibria between oxygen and aluminum and silicon respectively in liquid iron for various temperatures as well as the analyzed contents of the respective elements

Conclusions

Although the interaction between metal and the chosen slag systems leads to decreased contents of total oxygen in the steel, the main factor determining the final oxygen content is not clearly identifiable. The expected direct relation between the dissolved oxygen and aluminum contents in the metal and the alumina content of the slag are not sufficiently confirmed. Therfore, furhter detailled investigations are needed to identiefy the influence of fluorine on the oxygen activity of the slag and the corresponding equilibrium with the metal. Additionally the residual partial pressure of oxygen in the atmosphere needs to be considered with regard to the permeability of the various slag systems.

Summary

(1) In order to investigate the influence of various mixtures within the system CaF_2-CaO-Al_2O_3-MgO during slag treatment of a 21CrMoV5-7 steel, nine trials were performed in a vacuum induction furnace. Additionally, the refining behavior was studied for at least two different pressures.

(2) The conducted treatments with a pure oxide slag as well as with various mixtures of oxides and fluorides resulted in significantly reduced total oxygen contents in contrast to the input material.

(3) A pressure dependence of the final oxygen content was only observed by melting under a pure oxide slag.

(4) Due to the interaction between metal and slag a noticeable loss of silicon accompanied by an increase of the aluminum content was detected for most of the trials. Thereby, the degree of that interaction strongly depends on the fluoride content of the slag.

Outlook

In order to validate the findings derived from the trials where solely oxides were used as slag components these will be repeated. Furthermore, analysis with respect to the distribution of non-metallic inclusions using SEM-EDX methods as well as additional slag investigations will be carried out.
Subsequently, all present results will be compared to the behavior of 21CrMoV5-7 steel after electroslag remelting with similar slags and atmospheric conditions.

References

1. G. Klösch et al., “Nichtmetallische Einschlüsse in Langprodukten Entstehung, Bestimmung, Auswirkungen - ein Überblick,” *BHM Berg- und Hüttenmännische Monatshefte*, 154 (2009), 27-32
2. L. Zhang, and B.G. Thomas, “State of the Art in Evaluation and Control of Steel Cleanliness,” ISIJ International, 43 (2003), 271-291
3. N. Giesselmann, “Numerical simulation of the electroslag remelting process in order to determine influencing parameters on ingot defects,” *Proceedings of the 1st International Conference on Ingot Casting, Rolling and Forging*, (2012)
4. R. Schneider et al., “DESU-Prozessoptimierung zur Herstellung stickstofflegierter Stähle mit höchsten Reinheitsgraden“ *BHM Berg- und Hüttenmännische Monatshefte*, 147 (2002), 1-5
5. H. Schenck, and E. Steinmetz, “Wirkungsparameter von Begleitelementen in Eisenlösungen und ihre gegenseitigen Beziehungen,” *Stahleisen-Sonderberichte*, 7 (1968)
6. F. Oeters, “Metallurgie der Stahlherstellung,” *Springer Verlag*, (1989), 57-75
7. A. Mitchell, “Oxide inclusion behavior during consumable electrode remelting,” *Ironmaking and Steelmaking (Quarterly)*, 3 (1974), 172-179
8. K. Riyahimalayeri, P. Ölund, and M. Selleby, “Oxygen Activity Calculations of Molten Steel: Comparison With Measured Results,” *steel research international*, 84 (2013), 136-145
9. A. Mitchell, “Slag Functions in the ESR Process,” *Proceedings of the 2005 International Symposium in Liquid Metal Processing and Casting*, (2005)
10. GTT-Technologies, Herzogenrath, “FactSage 6.3”
11. K. Saito, R. Asano, and H. Matsuya “Enhancement of VSR Ingot Quality by Precise Melt Control,” *Electric Furnace Steel (Denki-Seiko)*, 80 (2009), 151-156
12. A. Sekiya, S. Nakayama, and T. Taketsuru “Deoxidation of Stainless Steel on Vacuum Electroslag Remelting Process,” *Electric Furnace Steel (Denki-Seiko)*, 66 (1995), 47-53